

Black Carbon Particles Do Not Matter for Immersion Mode Ice Nucleation

Journal Article**Author(s):**

Kanji, Zamin A ; Welte, André; Corbin, Joel C.; Mensah, Amewu A.

Publication date:

2020-06-16

Permanent link:

<https://doi.org/10.3929/ethz-b-000421473>

Rights / license:

[Creative Commons Attribution-NonCommercial 4.0 International](#)

Originally published in:

Geophysical Research Letters 47(11), <https://doi.org/10.1029/2019GL086764>

Funding acknowledgement:

150169 - Laboratory studies on the ice nucleation properties of fresh and aged mineral dust aerosols (SNF)

Geophysical Research Letters

RESEARCH LETTER

10.1029/2019GL086764

Key Points:

- Laboratory-generated black carbon and soot particles from hydrocarbon and fossil fuel do not nucleate ice at mixed-phase cloud conditions
- Homogeneous freezing temperatures are required for droplets containing soot to freeze
- Studies quantifying the aerosol contribution to ice nucleation do not need to include this INP type for temperatures warmer than 235 K

Correspondence to:

Z. A. Kanji,
zamin.kanji@env.ethz.ch

Citation:

Kanji, Z. A., Welti, A., Corbin, J. C., & Mensah, A. A. (2020). Black carbon particles do not matter for immersion mode ice nucleation. *Geophysical Research Letters*, 46, e2019GL086764. <https://doi.org/10.1029/2019GL086764>

Received 20 DEC 2019

Accepted 30 APR 2020

Accepted article online 3 MAY 2020

Black Carbon Particles Do Not Matter for Immersion Mode Ice Nucleation

Zamin A. Kanji¹ , André Welti^{1,2} , Joel C. Corbin^{1,3} , and Amewu A. Mensah^{1,4}

¹Institute for Atmospheric and Climate Science, ETH, Zurich, Zurich, Switzerland, ²Atmospheric Composition Unit, Finnish Meteorological Institute, Helsinki, Finland, ³Metrology Research Centre, National Research Council Canada, Ottawa, Canada, ⁴City of Zurich, Environment and Health Safety, Air Quality Research Division, Zurich, Switzerland

Abstract The role of black carbon (BC) in ice crystal formation via immersion freezing relevant for mixed-phase cloud formation is uncertain. Previous studies report either negligible or significant contributions of BC particles to cloud glaciation via immersion freezing. Despite conflicting evidence, immersion freezing by BC particles is included in several cloud models. Here we show that fossil fuel soot and commercially available hydrocarbon BC is inactive as immersion freezing nuclei for atmospherically relevant particle sizes and surface areas. Instead, temperatures <235 K are necessary for freezing droplets with immersed soot particles, implying homogeneous freezing, rather than immersion freezing by soot. A comparison of the results to previous studies using larger soot aggregates and dust reveals the ineffectiveness of soot as immersion ice nucleating particles. We conclude that soot particles with properties like those investigated here can be neglected for simulating ice nucleation in mixed-phase clouds.

Plain Language Summary Small subvisual particles in the atmosphere are responsible for cloud formation. Some of these particles, called ice nucleating particles (INPs), promote the freezing of individual cloud droplets. The chemical and physical properties that render particles INP are highly variable and poorly constrained. Here we show carbonaceous nanoparticles also called soot or black carbon, produced from various industrial processes and fossil fuel combustion do not contribute to ice crystal formation in clouds that form at temperatures between 0°C and −38°C unlike, for example, mineral dust. The findings suggest that climate and cloud models can neglect any contributions of soot to the formation of the ice phase in the atmosphere for temperatures greater than −38°C.

1. Introduction

Heterogeneous ice nucleation of carbonaceous nanoparticles, including black carbon (BC) containing particles like soot, is poorly constrained, making the role of BC particles in mixed-phase cloud (MPC) glaciation via primary ice formation highly uncertain (Bond et al., 2013; Hoose & Möhler, 2012; Kanji et al., 2017; Murray et al., 2012). A variety of freshly generated and chemically modified soot particles have been tested for their heterogeneous ice nucleation properties but yielded a scattered and unconstrained picture (summarized in Kanji et al., 2017). Some scatter in the results of soot ice nucleation can be explained by the variation in particle properties such as size, composition (due to combustion conditions), or morphology. Other differences arise from methodology or subjective and sometimes semiquantitative reporting of ice nucleation activity using selected parameters such as a threshold value. For example, reporting a single ice nucleation onset condition instead of the whole range of ice active fraction/frozen fraction (AF/FF) as a function of relative humidity (with respect to water, RH_w or ice, RH_i) or temperature (T). Such reporting has resulted in the chosen parameters being used as thresholds in cloud modeling studies (Karcher & Lohmann, 2003; Lohmann, 2002; Lohmann & Diehl, 2006) instead of a FF or AF as a function of T or RH , respectively.

Soot particles sourced from the combustion of hydrocarbons or fossil fuels have a complex morphology and composition, leading to a variety of characteristics that can affect ice nucleation. The type of fuel and combustion conditions used to produce BC containing particles for ice nucleation experiments have often been qualitatively correlated to their immersion freezing ability. Previous immersion freezing experiments reporting positive results on the ice nucleation ability of soot, investigated particles from acetylene combustion (DeMott, 1990), commercially available lamp black particles (Brooks et al., 2014; DeMott et al., 1999;

© 2020 The Authors.

This is an open access article under the terms of the Creative Commons Attribution-NonCommercial License, which permits use, distribution and reproduction in any medium, provided the original work is properly cited and is not used for commercial purposes.

Dymarska et al., 2006) or *n*-hexane soot (Dymarska et al., 2006). The fraction of 70–90 nm acetylene soot particles nucleating ice reached up to 3% at 238 K suggesting soot particles do contribute to ice formation at MPC relevant temperatures (235–273 K) (DeMott, 1990). Other studies investigating aging effects on ice nucleation with soot also reported positive results. For example, effects of ozone oxidation on the immersion freezing properties of lamp black soot particles showed average freezing at temperatures 2–3 K warmer than untreated soot, with a small fraction of soot particles causing freezing at temperatures as warm as 263 K (Brooks et al., 2014). In contrast to this, Dymarska et al. (2006) found no enhancement effect on the ice nucleation ability of lamp black soot particles exposed to ozone in the temperature range 242–258 K. However, the particle sizes used in the latter study were between 1 and 40 μm whereas in the former, agglomerates of average 137 μm in diameter were used. Both sizes call into question the relevance for atmospheric cloud formation since realistic atmospheric soot has a median diameter of 50–300 nm with number (mass) median size of 120 nm (200 nm) (Bond et al., 2013). The size of the investigated soot particles is decisive to the results of the experiments. At 253 K, small fractions of soot particles with mass median size up to 1 μm , produced from the combustion of benzene and toluene, were found to nucleate ice, and particles with oxidized functional groups were more active than those with hydrophobic surfaces (Gorbunov et al., 2001). Popovicheva et al. (2008) reported freezing of water droplets containing immersed soot particles at temperatures as warm as 265 K but state that the atmospheric relevance is limited because in their study numerous particles of soot were immersed in a single droplet that was being observed for freezing on a cold substrate. Recently, Vergara-Temprado et al. (2018) found that the ice nucleation active site (INAS) densities of soot particles produced from combustion of *n*-decane and eugenol ($\text{C}_{10}\text{H}_{12}\text{O}_2$) were significantly lower than those reported before for acetylene, lamp black, graphite spark, and combustion aerosol standard (CAST) soot. Low INAS density implies that only a small fraction of atmospherically relevant sized soot particles can nucleate ice, leading the authors to question whether ice nucleation from soot particles contribute to MPC glaciation. In Mahrt et al. (2018), the ice nucleation activity for black and brown carbon from propane combustion in a miniCAST burner, two types of lamp black soot, fullerene rich soot and carbon black soot, is reported in the temperature range 218–253 K. For $T > 235$ K, no ice nucleation activity was observed for a variety of relative humidity conditions including water saturated conditions relevant for immersion freezing. Similarly miniCAST BC soot also exhibited no detectable ice nucleation at 243 and 253 K (Friedman et al., 2011). Schill et al. (2018) report a negligible contribution of BC to immersion freezing at 243 K for an externally mixed particle population containing illite and snomax[®]. Furthermore, they report a decrease in ice nucleation activity when the BC was internally mixed with the particle population. Chou et al. (2013) also found no ice nucleation activity on fresh and photochemically aged diesel soot particles for $T > 235$ K, supporting a lack of contribution of soot particles to ice nucleation under MPC conditions.

In summary, the current state of knowledge suggests that for $T > 235$ K relevant for the MPC regime, combustion generated BC particles *could* contribute to ice nucleation in the MPC regime. However, experiments using particle or droplets sizes that are too large have limited atmospheric relevance. In this paper, we present immersion mode freezing results from experiments with single immersed soot aggregates of atmospherically relevant sizes (<400 nm) of five different BC samples including CAST black and brown carbon which have been used as a proxy for commercial jet engine exhaust emissions (Ess & Vasilatou, 2019; Marhaba et al., 2019).

2. Materials and Methods

Five different carbonaceous nanoparticle samples are investigated (see Table 1). The nanoparticles used in this study were produced as follows. Two soot samples were produced by a commercial propane-burning generator, the miniCAST model 00-4 as described in Corbin et al. (2014). One carbon black sample, Regal Black (Cabot Corp USA, lot # GP-3901) was nebulized and dried. Another carbon black sample, fullerene-enriched soot, was produced by heating graphite under Ar as described in Table 1. Finally, a spark generator was used to produce carbonaceous aggregates with a low degree of graphitization (PALAS Spark Generator, Gysel et al., 2012). These particles span a wide range of formation mechanisms, morphologies, and surface chemistries. Although they are not all strictly BC, we refer to them as such for simplicity herein. The particles, either dry generated or wet dispersed from an aqueous suspension, were fed into a mixing chamber to homogenize the particle concentrations and allow coagulation to increase the concentration of larger soot aggregates. The particles were then size selected in a differential mobility analyzer (DMA,

Table 1
Sources and Properties of Bc Samples used for Immersion Freezing Experiments

Sample type	Fuel source	Electrical mobility size selected (nm)	Other remarks
CAST black	^a Propane, CAST burner	100, 200, 400	Propane flame; C/O = 0.25, 10% thermal OC ^b
CAST brown	^a Propane CAST burner	200, 400	Quenched propane flame; C/O = 0.41, 30% thermal OC ^b
Spark generator	Graphite rods, PALAS Corp., Germany	100, 200, 400	Small monomer sizes, low degree of graphitization compared to soot. “diesel-like” morphology ^c
Regal black (nebulized from Milli-Q water)	Black pigment, Cabot Corp., USA (lot # GP-3901)	100, 200, 400	Surface-oxidized carbon black; widely used for SP-AMS calibration ^d
Fullerene-enriched soot (nebulized from in Milli-Q water)	Sigma-Aldrich (lot # MKBB8240V)	100, 200, 400	Produced by heating graphite under Ar; C ₆₀ and C ₇₀ (~6% and 1%) enriched graphitic carbon aggregates ^e . Used for SP2 Calibration ^f

^aCAST model 00-4, Jing Ltd., Zollikofen, Switzerland. ^bSchnaiter et al., 2006. ^cHelsper et al., 1993. ^dSoot particle aerosol mass spectrometer (Onasch et al., 2012). ^eKratschmer et al., 1990. ^fSingle particle soot photometer (Laborde et al., 2012).

TSI Inc., Model 3081) for their electrical mobility diameters. Monodisperse particles were introduced into the Immersion Mode Cooling Chamber (IMCA-ZINC, Lüönd et al., 2010) connected to the Zurich Ice Nucleation Chamber (ZINC, Stetzer et al., 2008). A schematic of the particle generation setup and immersion freezing experiment is shown in Figure 1.

The cloud chamber IMCA-ZINC has been characterized and used in previous ice nucleation studies (Boose et al., 2016; Hiranuma et al., 2015; Kanji et al., 2013; Lüönd et al., 2010; Welti et al., 2012; Welti et al., 2019) and thus is only briefly described here. In IMCA-ZINC, a particle flow of 0.6 l min⁻¹ containing dried BC particles is subjected to excessive RH_w of ~120% at $T \sim 303$ K for ~10 s allowing particles of all sizes and chemical properties to activate into cloud droplets of 18–20 μm in diameter. The activated cloud droplets cool in the transition from IMCA to the ZINC chamber and experience constant temperature and water saturation to prevent droplet evaporation. Frozen and liquid droplets are detected in situ after a residence time of ~10 s in ZINC, by the Ice Optical Depolarization Detector (IODE, see Figure 1) described in detail in Nicolet et al. (2010) and Lüönd et al. (2010). Counts of water droplets and ice crystals are used to determine the FF :

$$\text{frozen fraction (FF)} = \frac{\# \text{ice crystals}}{\#(\text{crystals} + \text{water droplets})} \quad (1)$$

Uncertainty in FF is estimated by quantifying the uncertainty in classification of liquid droplets as ice crystals and vice versa (see Lüönd et al., 2010 for a detailed analysis). At each experimental temperature, the FF is based on observations of ~3,000 particles, yielding an activation curve of FF versus temperature as shown in Figure 2. The FF of homogeneous freezing of 20 μm , pure water droplets (size of cloud droplets in IMCA-ZINC) is plotted in Figure 2 (gray shading) as a comparison. The FF for homogenous freezing is derived using the following equation:

$$FF = 1 - e^{-V \cdot t \cdot J_{\text{hom}}} \quad (2)$$

where V is the volume of a droplet with diameter 20 μm , $t = 10$ s (residence time in the supercooled region of IMCA-ZINC). J_{hom} is determined using Equation 18 of Ickes et al. (2015) using parameters for Fit 3 in Table 5 in Ickes et al. (2015). With our detection method, we are not able to resolve $FF < 0.05$ thus limiting the ice nucleation activity to particle properties present on more than 5% of the particles.

3. Results and Discussion

The FF as function of temperature and particle size of the five BC samples investigated (Table 1) are shown in Figure 2. All soot samples regardless of their source, O/C content, morphological properties, or aggregate size, require homogeneous freezing temperatures (gray shaded in area in Figure 2) for droplets to freeze. This indicates that the soot particles considered here are not detectably contributing to immersion freezing at the investigated temperatures, but freezing occurs only at a temperature regime where the homogeneous freezing rate of pure water droplets is high enough, regardless of the particle immersed in the droplets. By

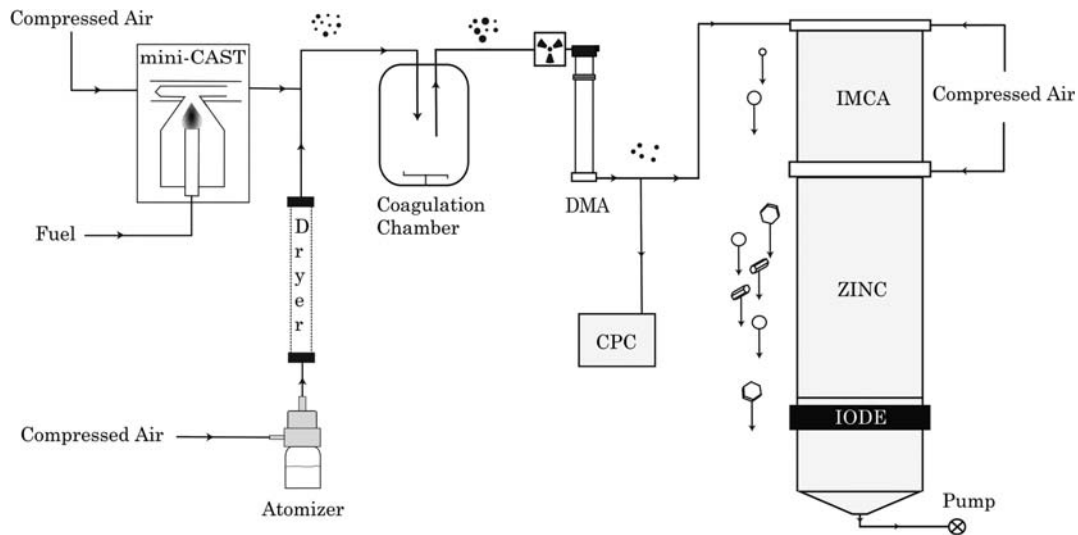


Figure 1. Schematic of experimental setup showing aerosol generation and ice nucleation, see text for acronyms.

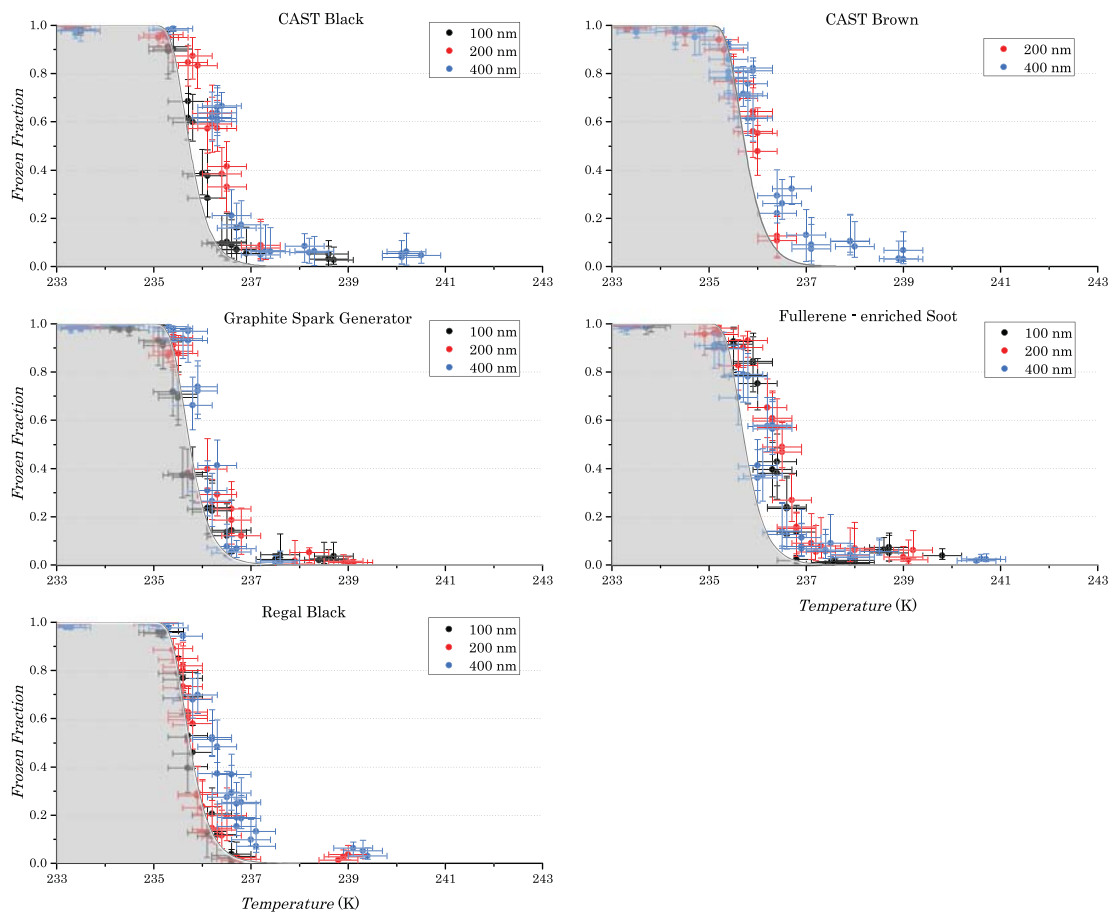


Figure 2. Immersion freezing results showing frozen fraction (FF) as a function of temperature, at water saturation for five BC samples. Homogeneous freezing probabilities shown as the gray shaded area are calculated for radius $10\ \mu\text{m}$ droplets and 10 s residence time. Homogeneous nucleation rates were derived from the parameterization (equation 18) of Ickes et al. (2015).

increasing the particle surface area (increasing the diameter or number of particles per droplet), freezing at higher temperatures (if any), could be possible if a small fraction of particles possess a rare occurring property that causes ice nucleation at higher temperatures. For example, freezing observed above 235 K for *n*-decane and eugenol soot in Vergara-Temprado et al. (2018) has been associated with a large surface area arising from soot particles with sizes of $>1 \mu\text{m}$ in the droplets, unrealistic for anthropogenic BC sources directly emitting large quantities of soot into the atmosphere. In urban emissions dominated by fossil fuel combustion both close to ground and in upper troposphere and lower stratosphere regions, mass median diameters of BC containing particles are reported to be 120–160 nm while number median diameters range from 50–80 nm (Bond et al., 2013). For biomass burning emissions, mass and number median diameters of up to 200 and 120 nm respectively are reported (Bond et al., 2013). The larger size in aged plumes resulting from coagulation after emission also does not produce particles on the order of microns (Bond et al., 2013). Soot particles from aviation emissions are reported to have mean diameters of 30 nm (Petzold et al., 2005). Producing large aggregates of microns in size would only be possible due to a substantial amount of coagulation (occurring only through large particle concentrations with longer mixing time scales in a constrained volume), which is unlikely to occur in the atmosphere, since plumes rapidly disperse after emission.

For the CAST brown sample, we did not perform 100 nm particle experiments because of the lack of freezing activity already observed for the 400 and 200 nm particles, seen as overlap of freezing temperatures with the homogenous freezing regime. The extreme hydrophobic nature of this type of soot required $RH_w > 140\%$ in IMCA to observe droplet activation. Absence of the soot aggregate-size dependence on the FF is a strong indication that the droplets did not freeze due to the soot surface within them, but by homogeneous freezing. The absence of size dependence of soot INPs at $T > 235 \text{ K}$ (sizes 100–400 nm) was also observed by Friedman et al. (2011) and Mahrt et al. (2018), in agreement with our conclusion that soot particles do not substantially contribute to heterogeneous ice nucleation under MPC conditions.

The samples investigated here cover a wide range of soot properties such as primary particle sizes, organic content, morphologies, and hydrophobicity (Corbin et al., 2014; Mahrt et al., 2018). This strongly suggests that any other types of soot or BC samples will not contradict the observation of an absence of heterogeneous freezing in the MPC temperature regime.

In Figure 3, we plot the median immersion freezing temperatures (T_{50} , the temperature at which the $FF = 0.5$) as a function of particle geometric surface area and diameter of the soot samples. As homogeneous freezing does not depend on the surface of immersed particles, we excluded plotting T_{50} for the cases where the $FF = 0.5$ data overlap (including uncertainties) with the homogeneous freezing regime shown in Figure 2 (gray shading). For comparison, the T_{50} as a function of soot particle surface area per droplet produced from *n*-decane and eugenol (Vergara-Temprado et al., 2018), acetylene soot (DeMott, 1990), kerosene soot (Diehl & Mitra, 1998), diesel soot (Schill et al., 2016), Cast soot (Ullrich et al., 2017), microcline particles (Atkinson et al., 2013; Welti et al., 2019), and natural desert dust particles (Niemand et al., 2012) are shown. BC containing particles in the atmosphere are predominantly in the Aitken and accumulation mode, mostly $\leq 200 \text{ nm}$ but can be up to 300 nm (Bond et al., 2013; Petzold et al., 1998; Petzold et al., 2005). Considering spherical particles $\leq 300 \text{ nm}$ (surface area $0.28 \mu\text{m}^2$, green shading Figure 3), the T_{50} is too low for soot to compete with homogeneous freezing of aqueous droplets, rendering heterogeneous freezing of BC negligible. By comparison, dust particles containing feldspar (microcline) with the same surface area would be active as INPs, as shown by the 10 K higher T_{50} . Similarly, the natural desert dust curve (N12 in Figure 3) has intermediate T_{50} between soot and feldspars but only for a dust particles larger than $0.3 \mu\text{m}$ (surface area $> 0.28 \mu\text{m}^2$). This is consistent with dust in the atmosphere, which typically ranges from $0.5\text{--}2 \mu\text{m}$ ($0.8\text{--}3 \mu\text{m}^2$) (Knippertz & Stuut, 2014) and freezes at significantly warmer temperatures than those required for soot or homogeneous ice nucleation.

Arguably, $0.28 \mu\text{m}^2$ based on the spherical geometrical surface area is an underestimate given the fractal nature of soot. Considering the Brunauer, Emmett, and Teller (BET; Brunauer et al., 1938) gas adsorption surface area of CAST black and measured single aggregate mass of different soot types found in the literature (Mahrt et al., 2018), a 300 nm particle can have surface area up to $0.5 \mu\text{m}^2$ (BET surface of $120 \text{ m}^2 \text{ g}^{-1}$, particle mass of 4 fg). The green- and red-hashed regions in Figure 3 show relevant surface areas within a cloud drop corresponding to particles $\leq 300 \text{ nm}$ derived from the geometric and BET surface area, respectively. We note that all studies showing soot to be an effective immersion INP with $T_{50} > 236 \text{ K}$ fall out of this hashed

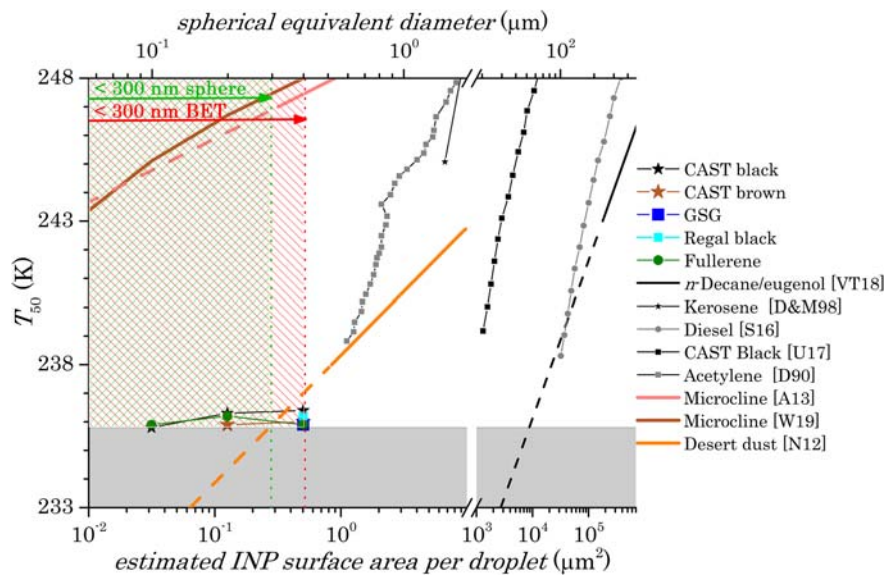


Figure 3. Median freezing temperature (T_{50}) as a function of INP surface area (bottom axis) and INP diameter (top axis). Gray-shaded area: region where 50% of droplets freeze homogeneously. In this region, freezing contribution of immersed particles is negligible. Any T_{50} overlapping with the homogeneous freezing curve is excluded. Hashed region: atmospherically relevant sizes of soot particles with geometric surface area of particles $\leq 300 \text{ nm}$ (green) and BET surface area for CAST black aggregates of $\leq 300 \text{ nm}$ equivalent mobility diameter. Dashed continuations of lines represent extrapolations. D90 (DeMott, 1990), D&M98 (Diehl & Mitra, 1998), N12 (Niemand et al., 2012), A13 (Atkinson et al., 2013), S16 (Schill et al., 2016), U17 (Ullrich et al., 2017), VT18 (Vergara-Temprado et al., 2018), and W19 (Welti et al., 2019).

region. The surface area per droplet required for soot particles to catalyze immersion freezing is larger than $\sim 1 \mu\text{m}^2$, corresponding to a size much larger ($\sim 600 \text{ nm}$) than found in the atmosphere (Bond et al., 2013 and references therein) or requiring multiple soot particles per droplet. The probability of having such large surface areas or aggregate sizes even after aging, coagulation (Bond et al., 2013) and accounting for wet scavenging, is extremely low (Ding et al., 2019), to the point of being impossible. In cases of extensive in-cloud wet scavenging and precipitation, residual soot particles were found with median diameters $< 240 \text{ nm}$ (Ding et al., 2019). The atmospherically relevant particle surface areas represented by the hashed region (even considering the fractal surface of soot, red region) demonstrates that soot particles will not have T_{50} high enough to compete with immersion freezing by dust or homogenous freezing. In summary, Figure 3 shows that for soot heterogeneous (immersion) freezing, surface areas larger than those of 600 nm particles are necessary within a cloud droplet; however, there is no observational evidence of such large airborne soot aggregates (surface area) (Bond et al., 2013).

A number of studies that used aerosolized single aggregate soot particles of atmospherically relevant sizes immersed in droplets of atmospherically relevant sizes (see Table 2) report negligible to no ice nucleation activity in the MPC temperature regime. However, significant ice nucleation in the cirrus regime at $T < 235 \text{ K}$ is reported in the same studies (Table 2). Studies reporting immersion freezing of soot using large

Table 2
Studies Reporting Ice Nucleation Abilities of Suspended Single Soot/BC Aggregates for $T > 235 \text{ K}$

Study	Soot type	Sampled MPC temperature range	Contribution or fraction of soot forming ice in the MPC regime
DeMott, 1990	Acetylene soot	$T > 238 \text{ K}$	Very weak ($AF = 0.06\%$ to 0.1% for high $RH_w = 101.4\text{--}102\%$) Strong contribution from homogeneous freezing $< 238 \text{ K}$
Friedman et al., 2011	Cast black (100, 200, and 400 nm)	253 and 243 K	No ice nucleation observed
Kanji et al., 2011	Graphite spark generator soot	$T < 243 \text{ K}$	No ice nucleation observed for $T > 234 \text{ K}$.
Chou et al., 2011	Diesel soot	243 and 238 K	No ice nucleation observed
Mahrt et al., 2018	Div. (6 samples, 100, 200, 300, and 400 nm)	238–253 K	No ice nucleation observed
This study (2020)	Div (5 samples, 100, 200, and 400 nm)	$T > 233 \text{ K}$	None, strong contribution from homogeneous freezing $< 236 \text{ K}$

surface areas per droplet from large aggregates or coagulated particles or using large droplet sizes (Brooks et al., 2014; Dymarska et al., 2006; Gorbunov et al., 2001; Popovicheva et al., 2008; Vergara-Temprado et al., 2018), have been excluded from Table 2. The data from the literature and from this study support the idea that soot particles derived from fossil and hydrocarbon fuel combustion are inactive INPs in the immersion freezing mode relevant to the MPC regime. We note that the results presented here are relevant for soot particles that are freshly emitted. However, organic acid coated (Friedman et al., 2011), photochemically aged (Schill et al., 2016) and cloud processed (Mahrt et al., 2020) soot particles also corroborate negligible ice nucleation activity at $T > 235$ K.

4. Conclusions

We present experiments on the immersion freezing ability of five different soot/BC types derived from the combustion of fossil and synthetic fuel sources and demonstrate that atmospherically relevant particle sizes of these soot types do not contribute to immersion freezing at $T > 235$ K. This is consistent with previous studies that used atmospherically relevant droplet and soot particle sizes. Contrary literature evidence suggesting soot particles can actively cause freezing at $T > 235$ K are from experiments using larger soot aggregates or particle numbers (i.e., surface areas) per droplet, thus representing atypical cases for the atmosphere. We acknowledge that atmospheric soot widely vary in properties and argue, the samples investigated in this work together with literature data cover a wide range of BC and soot formation mechanisms, morphologies and surface chemistries, representing a substantial body of negative results. The experimental findings strongly suggest that hydrocarbon and fossil fuel derived soot is inactive to immersion freezing at temperatures relevant for MPCs ($T > 235$ K). Based on this evidence, we recommend a careful review of parameterizations for immersion freezing with soot used in climate models. Future experiments could focus on characterizing soot particle properties and how they relate to ice nucleation in the cirrus regime, as there is evidence that soot particles contribute to deposition ice nucleation at $T < 235$ K (Kulkarni et al., 2016; Möhler et al., 2005; Nichman et al., 2019). Given that air traffic directly emits soot particles and water vapor at cirrus relevant altitudes, atmospheric processing of soot particles through contrail or homogeneous freezing of cloud droplets containing BC can occur. When the contrails sublime and release processed BC residuals, subsequent ice nucleation cycles could represent an important pathway of soot contributing to cirrus cloud formation (Mahrt et al., 2020).

Author Contribution

JCC and AAM built the soot generation setup and produced the samples. AW performed the immersion freezing measurements and analyzed the data. ZAK interpreted the data and prepared figures with contributions from AW. ZAK wrote the manuscript. All authors commented on the manuscript.

Acknowledgments

ZAK acknowledges funding from the ETH Atmospheric Physics Chair. AAM acknowledges funding from SNF grant 20020-152813, AW acknowledges funding from SNF grant 20020-150169, and JCC acknowledges funding from SNF grant 20021-132199. The authors acknowledge technical support from Hannes Wydler. The data presented in the publication are available online (<https://doi.org/10.3929/ethz-b-000406769>).

References

- Atkinson, J. D., Murray, B. J., Woodhouse, M. T., Whale, T. F., Baustian, K. J., Carslaw, K. S., et al. (2013). The importance of feldspar for ice nucleation by mineral dust in mixed-phase clouds. *Nature*, *498*(7454), 355–358. <https://doi.org/10.1038/nature12278>
- Bond, T. C., Doherty, S. J., Fahey, D. W., Forster, P. M., Berntsen, T., DeAngelo, B. J., et al. (2013). Bounding the role of black carbon in the climate system: A scientific assessment. *Journal of Geophysical Research: Atmospheres*, *118*, 5380–5552. <https://doi.org/10.1002/jgrd.50171>
- Boose, Y., Welti, A., Atkinson, J., Ramelli, F., Danielczok, A., Bingemer, H. G., et al. (2016). Heterogeneous ice nucleation on dust particles sourced from nine deserts worldwide—Part 1: Immersion freezing. *Atmospheric Chemistry and Physics*, *16*(23), 15,075–15,095. <https://doi.org/10.5194/acp-16-15075-2016>
- Brooks, S. D., Suter, K., & Olivarez, L. (2014). Effects of chemical aging on the ice nucleation activity of soot and polycyclic aromatic hydrocarbon aerosols. *Journal of Physical Chemistry A*, *118*(43), 10,036–10,047. <https://doi.org/10.1021/jp508809y>
- Brunauer, S., Emmett, P. H., & Teller, E. (1938). Adsorption of gases in multimolecular layers. *Journal of the American Chemical Society*, *60*, 309–319. <https://doi.org/10.1021/ja01269a023>
- Chou, C., Kanji, Z. A., Stetzer, O., Tritscher, T., Chirico, R., Heringa, M. F., et al. (2013). Effect of photochemical ageing on the ice nucleation properties of diesel and wood burning particles. *Atmospheric Chemistry and Physics*, *13*(2), 761–772. <https://doi.org/10.5194/acp-13-761-2013>
- Chou C., Stetzer O., Weingartner E., Jurányi Z., Kanji Z. A., Lohmann U. (2011). Ice nuclei properties within a Saharan dust event at the Jungfrauoch in the Swiss Alps. *Atmospheric Chemistry and Physics*, *11*(10), 4725–4738. <https://doi.org/10.5194/acp-11-4725-2011>
- Corbin, J. C., Sierau, B., Gysel, M., Laborde, M., Keller, A., Kim, J., et al. (2014). Mass spectrometry of refractory black carbon particles from six sources: Carbon-cluster and oxygenated ions. *Atmospheric Chemistry and Physics*, *14*(5), 2591–2603. <https://doi.org/10.5194/acp-14-2591-2014>
- DeMott, P. J. (1990). An exploratory-study of ice nucleation by soot aerosols. *Journal of Applied Meteorology*, *29*(10), 1072–1079.

- DeMott, P. J., Chen, Y., Kreidenweis, S. M., Rogers, D. C., & Sherman, D. E. (1999). Ice formation by black carbon particles. *Geophysical Research Letters*, *26*(16), 2429–2432.
- Diehl, K., & Mitra, S. K. (1998). A laboratory study of the effects of a kerosene-burner exhaust on ice nucleation and the evaporation rate of ice crystals. *Atmospheric Environment*, *32*(18), 3145–3151. [https://doi.org/10.1016/s1352-2310\(97\)00467-6](https://doi.org/10.1016/s1352-2310(97)00467-6)
- Ding, S., Zhao, D., He, C., Huang, M., He, H., Tian, P., et al. (2019). Observed interactions between black carbon and hydrometeor during wet scavenging in mixed-phase clouds. *Geophysical Research Letters*, *46*, 8453–8463. <https://doi.org/10.1029/2019GL083171>
- Dymarska, M., Murray, B. J., Sun, L. M., Eastwood, M. L., Knopf, D. A., & Bertram, A. K. (2006). Deposition ice nucleation on soot at temperatures relevant for the lower troposphere. *Journal of Geophysical Research*, *111*, D04204. <https://doi.org/10.1029/2005JD006627>
- Ess, M. N., & Vasilatou, K. (2019). Characterization of a new miniCAST with diffusion flame and premixed flame options: Generation of particles with high EC content in the size range 30 nm to 200 nm. *Aerosol Science and Technology*, *53*(1), 29–44. <https://doi.org/10.1080/02786826.2018.1536818>
- Friedman, B., Kulkarni, G., Beranek, J., Zelenyuk, A., Thornton, J. A., & Cziczko, D. J. (2011). Ice nucleation and droplet formation by bare and coated soot particles. *Journal of Geophysical Research*, *116*, D17203. <https://doi.org/10.1029/2011JD015999>
- Gorbunov, B., Baklanov, A., Kakutkina, N., Windsor, H. L., & Toumi, R. (2001). Ice nucleation on soot particles. *Journal of Aerosol Science*, *32*(2), 199–215. [https://doi.org/10.1016/S0021-8502\(00\)00077-X](https://doi.org/10.1016/S0021-8502(00)00077-X)
- Gysel, M., Laborde, M., Mensah, A. A., Corbin, J. C., Keller, A., Kim, J., et al. (2012). Technical note: The single particle soot photometer fails to reliably detect PALAS soot nanoparticles. *Atmospheric Measurement Techniques*, *5*(12), 3099–3107. <https://doi.org/10.5194/amt-5-3099-2012>
- Helsper, C., Molter, W., Löffler, F., Wadenpohl, C., Kaufmann, S., & Wenninger, G. (1993). Investigations of a new aerosol generator for the production of carbon aggregate particles. *Atmospheric Environment Part a-General Topics*, *27*(8), 1271–1275. [https://doi.org/10.1016/0960-1686\(93\)90254-v](https://doi.org/10.1016/0960-1686(93)90254-v)
- Hiranuma, N., Augustin-Bauditz, S., Bingemer, H., Budke, C., Curtius, J., Danielczok, A., et al. (2015). A comprehensive laboratory study on the immersion freezing behavior of illite NX particles: a comparison of 17 ice nucleation measurement techniques. *Atmospheric Chemistry and Physics*, *15*(5), 2489–2518. <https://doi.org/10.5194/acp-15-2489-2015>
- Hoese, C., & Möhler, O. (2012). Heterogeneous ice nucleation on atmospheric aerosols: a review of results from laboratory experiments. *Atmospheric Chemistry and Physics*, *12*(20), 9817–9854. <https://doi.org/10.5194/acp-12-9817-2012>
- Ickes, L., Welti, A., Hoese, C., & Lohmann, U. (2015). Classical nucleation theory of homogeneous freezing of water: thermodynamic and kinetic parameters. *Physical Chemistry Chemical Physics*, *17*(8), 5514–5537. <https://doi.org/10.1039/C4CP04184D>
- Kanji Z. A., DeMott P. J., Möhler O., Abbatt J. P. D. (2011). Results from the University of Toronto continuous flow diffusion chamber at ICIS 2007: instrument intercomparison and ice onsets for different aerosol types. *Atmospheric Chemistry and Physics*, *11*(1), 31–41. <https://doi.org/10.5194/acp-11-31-2011>
- Kanji, Z. A., Ladino, L. A., Wex, H., Boose, Y., Burkert-Kohn, M., Cziczko, D. J., & Krämer, M. (2017). Overview of ice nucleating particles. *Meteorological Monographs*, *58*, 1.1–1.33. <https://doi.org/10.1175/AMSMONOGRAPH-D-16-0006.1>
- Kanji, Z. A., Welti, A., Chou, C., Stetzer, O., & Lohmann, U. (2013). Laboratory studies of immersion and deposition mode ice nucleation of ozone aged mineral dust particles. *Atmospheric Chemistry and Physics*, *13*(17), 9097–9118. <https://doi.org/10.5194/acp-13-9097-2013>
- Karcher, B., & Lohmann, U. (2003). A parameterization of cirrus cloud formation: Heterogeneous freezing. *Journal of Geophysical Research*, *108*(D14), 4402. <https://doi.org/10.1029/2002JD003220>
- Knippertz, P., & Stuu, J. B. W. (2014). *Mineral dust: A key player in the earth system*. Netherlands: Springer.
- Kratschmer, W., Fostiropoulos, K., & Huffman, D. R. (1990). The infrared and ultraviolet-absorption spectra of laboratory-produced carbon dust—Evidence for the presence of the C-60 molecule. *Chemical Physics Letters*, *170*(2-3), 167–170. [https://doi.org/10.1016/0009-2614\(90\)87109-5](https://doi.org/10.1016/0009-2614(90)87109-5)
- Kulkarni, G., China, S., Liu, S., Nandasiri, M., Sharma, N., Wilson, J., et al. (2016). Ice nucleation activity of diesel soot particles at cirrus relevant temperature conditions: Effects of hydration, secondary organics coating, soot morphology, and coagulation. *Geophysical Research Letters*, *43*, 3580–3588. <https://doi.org/10.1002/2016GL068707>
- Laborde, M., Mertes, P., Zieger, P., Dommen, J., Baltensperger, U., & Gysel, M. (2012). Sensitivity of the single particle soot photometer to different black carbon types. *Atmospheric Measurement Techniques*, *5*(5), 1031–1043. <https://doi.org/10.5194/amt-5-1031-2012>
- Lohmann, U. (2002). A glaciation indirect aerosol effect caused by soot aerosols. *Geophysical Research Letters*, *29*(4), 1052. <https://doi.org/10.1029/2001gl014357>
- Lohmann, U., & Diehl, K. (2006). Sensitivity studies of the importance of dust ice nuclei for the indirect aerosol effect on stratiform mixed-phase clouds. *Journal of the Atmospheric Sciences*, *63*(3), 968–982. <https://doi.org/10.1175/jas3662.1>
- Lüönd, F., Stetzer, O., Welti, A., & Lohmann, U. (2010). Experimental study on the ice nucleation ability of size-selected kaolinite particles in the immersion mode. *Journal of Geophysical Research*, *115*, D14201. <https://doi.org/10.1029/2009JD012959>
- Mahrt, F., Kilchhofer, K., Marcolli, C., Grönquist, P., David, R. O., Rösch, M., et al. (2020). The impact of cloud processing on the ice nucleation abilities of soot particles at cirrus temperatures. *Journal of Geophysical Research: Atmospheres*, *125*, e2019JD030922. <https://doi.org/10.1029/2019JD030922>
- Mahrt, F., Marcolli, C., David, R. O., Grönquist, P., Barthazy Meier, E. J., Lohmann, U., & Kanji, Z. A. (2018). Ice nucleation abilities of soot particles determined with the Horizontal Ice Nucleation Chamber. *Atmospheric Chemistry and Physics*, *18*(18), 13,363–13,392. <https://doi.org/10.5194/acp-18-13363-2018>
- Marhaba, I., Ferry, D., Laffon, C., Regier, T. Z., Ouf, F. X., & Parent, P. (2019). Aircraft and MiniCAST soot at the nanoscale. *Combustion and Flame*, *204*, 278–289. <https://doi.org/10.1016/j.combustflame.2019.03.018>
- Möhler, O., Linke, C., Saathoff, H., Schnaiter, M., Wagner, R., Mangold, A., et al. (2005). Ice nucleation on flame soot aerosol of different organic carbon content. *Meteorologische Zeitschrift*, *14*(4), 477–484.
- Murray, B. J., O'Sullivan, D., Atkinson, J. D., & Webb, M. E. (2012). Ice nucleation by particles immersed in supercooled cloud droplets. *Chemical Society Reviews*, *41*(19), 6519–6554. <https://doi.org/10.1039/c2cs35200a>
- Nichman, L., Wolf, M., Davidovits, P., Onasch, T. B., Zhang, Y., Worsnop, D. R., et al. (2019). Laboratory study of the heterogeneous ice nucleation on black-carbon-containing aerosol. *Atmospheric Chemistry and Physics*, *19*(19), 12,175–12,194. <https://doi.org/10.5194/acp-19-12175-2019>
- Nicolet, M., Stetzer, O., Lüönd, F., Möhler, O., & Lohmann, U. (2010). Single ice crystal measurements during nucleation experiments with the depolarization detector IODE. *Atmospheric Chemistry and Physics*, *10*(2), 313–325. <https://doi.org/10.5194/acp-10-313-2010>
- Niemand, M., Möhler, O., Vogel, B., Vogel, H., Hoese, C., Connolly, P., et al. (2012). A particle-surface-area-based parameterization of immersion freezing on desert dust particles. *Journal of the Atmospheric Sciences*, *69*(10), 3077–3092. <https://doi.org/10.1175/jas-d-11-0249.1>

- Onasch, T. B., Trimborn, A., Fortner, E. C., Jayne, J. T., Kok, G. L., Williams, L. R., et al. (2012). Soot particle aerosol mass spectrometer: Development, validation, and initial application. *Aerosol Science and Technology*, *46*(7), 804–817. <https://doi.org/10.1080/02786826.2012.663948>
- Petzold, A., Gysel, M., Vancassel, X., Hitzemberger, R., Puxbaum, H., Vrochiticky, S., et al. (2005). On the effects of organic matter and sulphur-containing compounds on the CCN activation of combustion particles. *Atmospheric Chemistry and Physics*, *5*, 3187–3203. <https://doi.org/10.5194/acp-5-3187-2005>
- Petzold, A., Strom, J., Ohlsson, S., & Schroder, F. P. (1998). Elemental composition and morphology of ice-crystal residual particles in cirrus clouds and contrails. *Atmospheric Research*, *49*(1), 21–34. [https://doi.org/10.1016/s0169-8095\(97\)00083-5](https://doi.org/10.1016/s0169-8095(97)00083-5)
- Popovicheva, O., Kireeva, E., Persiantseva, N., Khokhlova, T., Shonija, N., Tishkova, V., & Demirdjian, B. (2008). Effect of soot on immersion freezing of water and possible atmospheric implications. *Atmospheric Research*, *90*(2–4), 326–337. <https://doi.org/10.1016/j.atmosres.2008.08.004>
- Schill, G. P., DeMott, P. J., Levin, E. J. T., & Kreidenweis, S. M. (2018). Use of the Single Particle Soot Photometer (SP2) as a pre-filter for ice nucleation measurements: Effect of particle mixing state and determination of SP2 conditions to fully vaporize refractory black carbon. *Atmospheric Measurement Techniques*, *11*(5), 3007–3020. <https://doi.org/10.5194/amt-11-3007-2018>
- Schill, G. P., Jathar, S. H., Kodros, J. K., Levin, E. J. T., Galang, A. M., Friedman, B., et al. (2016). Ice-nucleating particle emissions from photochemically aged diesel and biodiesel exhaust. *Geophysical Research Letters*, *43*, 5524–5531. <https://doi.org/10.1002/2016GL069529>
- Schnaiter, M., Gimmler, M., Llamas, I., Linke, C., Jäger, C., & Mutschke, H. (2006). Strong spectral dependence of light absorption by organic carbon particles formed by propane combustion. *Atmospheric Chemistry and Physics*, *6*, 2981–2990. <https://doi.org/10.5194/acp-6-2981-2006>
- Stetzer, O., Baschek, B., Luond, F., & Lohmann, U. (2008). The Zurich Ice Nucleation Chamber (ZINC)—A new instrument to investigate atmospheric ice formation. *Aerosol Science and Technology*, *42*(1), 64–74. <https://doi.org/10.1080/02786820701787944>
- Ullrich, R., Hoose, C., Möhler, O., Niemand, M., Wagner, R., Höhler, K., et al. (2017). A new ice nucleation active site parameterization for desert dust and soot. *Journal of the Atmospheric Sciences*, *74*(3), 699–717. <https://doi.org/10.1175/JAS-D-16-0074.1>
- Vergara-Temprado, J., Holden Mark, A., Orton Thomas, R., O'Sullivan, D., Umo Nsikanabasi, S., Browne, J., et al. (2018). Is black carbon an unimportant ice-nucleating particle in mixed-phase clouds? *Journal of Geophysical Research: Atmospheres*, *123*, 4273–4283. <https://doi.org/10.1002/2017JD027831>
- Welti, A., Lohmann, U., & Kanji, Z. A. (2019). Ice nucleation properties of K-feldspar polymorphs and plagioclase feldspars. *Atmospheric Chemistry and Physics*, *19*(16), 10,901–10,918. <https://doi.org/10.5194/acp-2018-1271>
- Welti, A., Lüönd, F., Kanji, Z. A., Stetzer, O., & Lohmann, U. (2012). Time dependence of immersion freezing: an experimental study on size selected kaolinite particles. *Atmospheric Chemistry and Physics*, *12*(20), 9893–9907. <https://doi.org/10.5194/acp-12-9893-2012>